

Modeling local predictive ability using power-transformed Gaussian processes

Oscar Oelrich^{a*} and Mattias Villani^{a,b}

^aDepartment of Statistics, Stockholm University

^bDepartment of Computer and Information Science, Linköping University

A Gaussian process is proposed as a model for the posterior distribution of the local predictive ability of a model or expert, conditional on a vector of covariates, from historical predictions in the form of log predictive scores. Assuming Gaussian expert predictions and a Gaussian data generating process, a linear transformation of the predictive score follows a noncentral chi-squared distribution with one degree of freedom. Motivated by this we develop a non-central chi-squared Gaussian process regression to flexibly model local predictive ability, with the posterior distribution of the latent GP function and kernel hyperparameters sampled by Hamiltonian Monte Carlo. We show that a cube-root transformation of the log scores is approximately Gaussian with homoscedastic variance, which makes it possible to estimate the model much faster by marginalizing the latent GP function analytically. Linear pools based on learned local predictive ability are applied to predict daily bike usage in Washington DC.

1. Introduction

The out-of-sample predictive accuracy of an *expert*, which could be a formal model or an opinionated human, is typically treated as a fixed quantity to be estimated (Gelman et al., 2014). Our aim here is to model *local predictive ability*, i.e. predictive ability as a function of a vector of covariates \mathbf{z} , to capture how the predictive abilities of a set of experts vary over the space of \mathbf{z} (Yao et al., 2021; Li et al., 2021; Oelrich et al., 2021).

*Corresponding author: oscar.oelrich@stat.su.se. The computations in this paper were enabled by resources in project SNIC 2020/15-262 provided by the Swedish National Infrastructure for Computing (SNIC) at UPPMAX, partially funded by the Swedish Research Council through grant agreement no. 2018-05973.

We aim to obtain the posterior distribution of the local predictive ability to properly quantify the uncertainty of the expert’s predictive ability.

Since measures of predictive ability of experts can be used to combine, or pool, expert predictions (Bates and Granger, 1969; Hall and Mitchell, 2007; Geweke and Amisano, 2011; Yao et al., 2018), we call the space spanned by this vector the *pooling space* (Oelrich et al., 2021) and the variables in \mathbf{z} *pooling variables*. The choice of pooling variables is determined by the *decision maker* (Lindley et al., 1979) making the aggregated prediction, based on what she believes are important determinants of the experts’ local predictive abilities.

Our focus is on the accuracy of an expert’s forecast *density* (Gelman et al., 2014). Density forecasts are typically part of the output from probabilistic models, but are also increasingly reported from human experts. For example, the histogram densities for key macroeconomic variables from the Survey of Professional Forecasters conducted by the Federal Reserve Bank of Philadelphia for the US (Croushore et al., 2019) and the European Central Bank for the Euro Area (de Vincent-Humphreys et al., 2019) or probabilistic forecasts of temperature and precipitation in meteorology from a combination of subjective experts, historical data and complex deterministic scientific models (AMS Council, 2008).

A theoretically motivated measure of predictive ability is the expected log predictive density (ELPD), which can be unbiasedly estimated by the average log predictive density evaluations (log scores) on a test dataset. The distribution of the log scores is typically complex however (Sivula et al., 2022b), making inferences for ELPD challenging. The likelihood of the observed log scores depends not only on the model/expert but also on the data-generating process (DGP). For example, using a simple model with additive noise will typically work poorly, as when the predictive distribution and the DGP are normal, the log scores will follow a scaled and translated noncentral χ_1^2 distribution (Sivula et al., 2022a).

Further, specifying a model for the relationship between all the covariates and predictive ability is a challenging problem in itself. Certain variables may be expected to be important for predictive ability but the exact functional form to use to model this relationship may be harder to pinpoint. In a situation of little prior information it makes sense for the decision maker to go with a non-parametric model that can capture variations in predictive ability over an arbitrary pooling space in a flexible manner. Oelrich et al. (2021) propose the non-parametric caliper estimator of local predictive ability, which works by averaging log scores locally in pooling space. The caliper estimator is flexible, but has the potential drawback that the inferred local ability surface is discontinuous, and the lack of smoothness may result in large variability for the local estimates.

We here propose a flexible noncentral χ^2 Gaussian process (GP) regression, where the latent GP surface models the conditional ELPD over the space of pooling variables in \mathbf{z} . A Gaussian process explicitly models the correlation properties, but other than that makes minimal assumptions about the specific relationship between the covariates and the ELPD. The smoothness and other hyperparameters in the covariance kernel are assumed unknown and are inferred jointly with the latent GP surface. A Gaussian

process model for local ELPD is attractive since it gives a direct quantification of the uncertainty about the underlying ELPD surface for each expert.

The joint posterior distribution of the conditional ELPD and kernel hyperparameters are sampled by Hamiltonian Monte Carlo (HMC) using Stan (Stan Development Team, 2022). The dimension of the sampled conditional ELPD grows with the sample size however, and inferences are time-consuming even for moderately large datasets. We show empirically that a cube-root transformation of the log scores is approximately Gaussian with homoscedastic variance. This makes it possible to integrate out the latent GP surface analytically and sample the low-dimensional marginal posterior kernel hyperparameters by HMC, which is much faster and scalable for larger datasets. We show that the ELPD surface can then be easily sampled by standard GP methods (Rasmussen and Williams, 2006, Chapter 2) combined with analytically available third moments of Gaussian processes. In the more general case when either the expert or the data generating process is non-Gaussian we propose to use a general power transformation of the ELPD and to estimate the power transformation using HMC jointly with the kernel hyperparameters.

The paper proceeds as follows. Section 2 defines local predictive ability and describes the non-central χ^2 Gaussian process (GP) regression for estimating it, along with the computationally more efficient GP regression on power-transformed log scores. Section 3 illustrates these methods using a simple simulation study. Section 4 consists of an empirical example analyzing local predictive ability for a set of models in a bike sharing dataset. Section 5 concludes.

2. A framework for estimating local predictive ability

2.1. Local predictive ability

We consider the problem where a decision maker is presented with a set of K experts, either in the form of models or opinionated humans, and wants to estimate how well the experts make predictions, based on their historical performance. We assume that the decision maker has access to historic predictions made by the experts in the form of log predictive density scores $\ell_{ik} = \log p_k(y_i | \mathbf{y}_k)$, assessing the prediction of observation y_i in the k th expert’s predictive density given a set of training data \mathbf{y}_k . While nothing prevents us from considering other measures, such as mean squared error, the derived model for predictive ability depends on the chosen measure. The log predictive density score is considered the gold standard for measuring predictive performance since it has the unique advantage of being both local and proper (Gneiting and Raftery, 2007), and is therefore commonly used in model selection. Further, the expected log predictive density of a predictive distribution is proportional to the Kullback-Leibler divergence with regards to the data-generating process (Hall and Mitchell, 2007).

The decision maker uses the expected log predictive density for a new data point \tilde{y} from the data-generating process $p_*(y)$ to measure the predictive ability of expert k

$$\eta_k \equiv \mathbb{E}_{p_*(y)} [\log p_k(\tilde{y} | \mathbf{y}_k)] = \int_{-\infty}^{\infty} [\log p_k(\tilde{y} | \mathbf{y})] p_*(y) dy, \quad (1)$$

where \tilde{y} is a new (out-of sample) observation, $p_*(\cdot)$ is the density of the data-generating process, and \mathbf{y}_k is the training data the expert has access to. The variable of interest, y , can be univariate or multivariate, but we will for simplicity assume that it is univariate here.

The decision maker further believes that the predictive ability of the experts vary over a set of pooling variables (Oelrich et al., 2021). She is therefore not only interested in determining how good the experts are at making predictions in general, but how good they are at making predictions conditional on a vector of pooling variables, \mathbf{z} . We call this conditional predictive ability the *local predictive ability* of the expert at \mathbf{z}

$$\eta_k(\mathbf{z}) \equiv \mathbb{E}_{p_*(\tilde{y})} [\log p(\tilde{y} | \mathbf{y}_k, \mathbf{z})] = \int_{-\infty}^{\infty} [\log p(\tilde{y} | \mathbf{y}_k, \mathbf{z})] p_*(y) dy. \quad (2)$$

2.2. Distribution of the log scores

The log scores of the experts, ℓ_{ik} for $k = 1, \dots, K$ and $i = 1, \dots, n$, are treated as data by the decision maker (Lindley et al., 1979) from which she infers how the ELPD varies over the pooling space. The choice of pooling variables is therefore a pure modeling problem from the viewpoint of the decision maker. The decision maker does not need to know if the experts have access to the pooling variables when making their predictions, but this information can of course affect the modeling choices of the decision maker.

The correct model for local predictive ability is determined by the predictive distribution of the expert, which is typically known, and the data-generating process, which is typically unknown. In order to specify a parametric model for the log scores, we therefore need access to the predictive distribution of the expert. Different predictive distribution will lead to different models of local predictive ability.

Consider the practically important scenario where the expert predictive distributions, as well as the data generating process, are all Gaussian. Specifically, let the predictive distribution of expert k for the data point y_i be $y_i | \mathbf{y} \sim \mathcal{N}(\mu_{ik}, \sigma_{ik}^2)$, where \mathbf{y} is the training data used by the expert. The log score is then

$$\ell_{ik} \equiv \log p_k(y_i | \mathbf{y}) = -\frac{1}{2} \log(2\pi\sigma_{ik}^2) - \frac{1}{2\sigma_{ik}^2} (y_i - \mu_{ik})^2. \quad (3)$$

If we let the data-generating process be given by $y_i \sim \mathcal{N}(\mu_{i*}, \sigma_{i*}^2)$, we can rewrite Equation (3) as

$$\ell_{ik} \equiv \log p_k(y_i) = -\frac{1}{2} \log(2\pi\sigma_{ik}^2) - \frac{\sigma_{i*}^2}{2\sigma_{ik}^2} \left(\frac{y_i - \mu_{ik}}{\sigma_{i*}} \right)^2, \quad (4)$$

and since $(y_i - \mu_{ik})/\sigma_{i*} \sim \mathcal{N}(\mu_{i*} - \mu_{ik}, 1)$, it follows that (Sivula et al., 2022a)

$$\ell_{ik} \stackrel{d}{=} a_{ik} - b_{ik} \cdot X_{ik}, \quad (5)$$

where $X_{ik} \sim \chi_1^2(\lambda_{ik})$ with non-centrality parameter $\lambda_{ik} = (\mu_{i*} - \mu_{ik})^2/\sigma_{i*}^2$, $a_{ik} = -\frac{1}{2} \log(2\pi\sigma_{ik}^2)$ and $b_{ik} = \sigma_{i*}^2/(2\sigma_{ik}^2)$. Hence, the noncentrality parameter λ_{ik} depends

on the difference between the predictive mean of the expert and the mean of the data-generating process; the shape of the distribution of the log scores therefore varies dramatically with $\mu_{i*} - \mu_{ik}$ and is typically highly non-Gaussian for all b , see Figure 1 for an illustration.

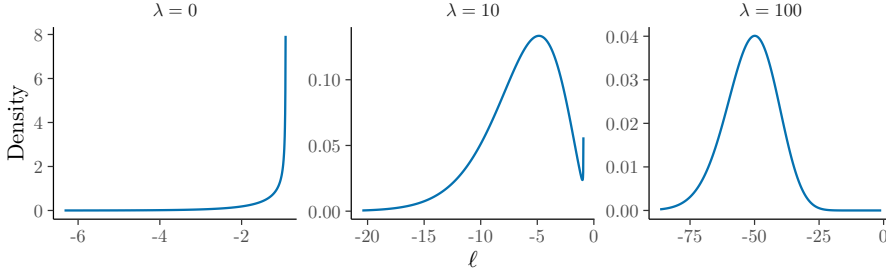


Figure 1: Distribution of log scores for a Gaussian expert and DGP with equal variance for three different $\lambda_k = (\mu_{i*} - \mu_{ik})^2$.

Since $a_{ik} = -\frac{1}{2} \log(2\pi\sigma_{ik}^2)$ only depends on the expert’s predictive distribution and is therefore assumed known, we can define $\ell'_{ik} \equiv -(\ell_{ik} - a_{ik})$ and write the model in (5) as

$$\ell'_{ik} \mid \lambda_{ik}, b_{ik} \sim \chi_1^2(\lambda_{ik}, b_{ik}), \quad (6)$$

where $\chi_1^2(\lambda, b)$ denotes a *scaled* non-central χ^2 with one degree of freedom, non-centrality parameter λ and scale parameter b . A useful simplification of the model in (6) is to assume that $b_{ik} = b_k$ for all $i = 1, \dots, n$, i.e. that the variance ratio $\sigma_{i*}^2/\sigma_{ik}^2$ is constant over observations for a given expert.

2.3. Scaled non-central χ^2 Gaussian process regression

The setup with Gaussian data generating process and experts in the previous subsection suggests a scaled non-central χ^2 regression for modeling the local predictive ability of experts. We will here propose a nonparametric Bayesian model where the log of the noncentrality parameter is modeled by a Gaussian process over the pooling space.

A Gaussian process (GP) generalizes the Gaussian distribution from a random variable to a stochastic process (Rasmussen and Williams, 2006). In simple terms, a Gaussian process is an infinite sequence of function values with different inputs $\{f(\mathbf{z}_1), f(\mathbf{z}_2), f(\mathbf{z}_3), \dots\}$, any subset of which follows a multivariate Gaussian distribution. Each GP has a covariance function, or kernel, which depends on the input values and specifies how the covariance matrix for each subset of the sequence should be constructed. The specific covariance function we select determines our prior regarding how smoothly the outputs vary over the input space. The covariance function we use in the examples and applications in this paper is called the squared exponential with automatic relevance determination (ARD) (Neal, 1996)

$$k_{\text{SE}}(\mathbf{z}_i, \mathbf{z}_j) = \alpha^2 \exp\left(-\frac{1}{2}(\mathbf{z}_i - \mathbf{z}_j)(\text{diag}(\mathbf{l})^{-2})(\mathbf{z}_i - \mathbf{z}_j)\right) + \delta_{ij}\sigma_n^2, \quad (7)$$

where \mathbf{l} is a vector of *length scales*, α denotes the signal standard deviation, σ_n^2 denotes the noise variance, and δ_{ij} is the Kronecker function, which takes the value 1 when $i = j$ and 0 otherwise. Kernels where the length scales of different inputs are allowed to differ are referred to as automatic relevance determination kernels, as the length scales are inversely related to relevance (Rasmussen and Williams, 2006).

as the length scale determines how quickly we assume the function values to vary with regards to a specific input, and the more smoothly the function value varies with regards to a specific input, the more relevant that input can be considered.

Our non-central χ^2 Gaussian process model for the log scores is

$$\begin{aligned} \ell'_{ik} \mid \lambda_k(\mathbf{z}_i), b_k &\stackrel{\text{indep.}}{\sim} \chi_1^2(\lambda_k(\mathbf{z}_i), b_k) \\ \log \lambda_k(\mathbf{z}) &\sim \text{GP}(\mu_k(\mathbf{z}), g_k(\mathbf{z}, \mathbf{z}')) \\ b_k &\sim \mathcal{N}^+(1/2, \psi_b^2), \end{aligned} \tag{8}$$

where $\mathcal{N}^+(\cdot, \cdot)$ denotes a normal distribution truncated at 0. Note that $b_k > 0$, and $b_k = 1/2$ when the variance of the DGP and the expert match. Further, note that the GP is on the log of the noncentrality parameter, ensuring that $\lambda_k(\mathbf{z})$ stays non-negative. Since the mean of a $\chi_1^2(\lambda, b)$ variable is $b(1 + \lambda)$, the Gaussian process in (8) directly implies a flexible prior for the mean function of the log scores, i.e. the local ELPD. We will refer to the model in (8) as $\text{GP}(\chi_1^2)$. The mean function $\mu_k(\cdot)$ and the covariance kernel $g_k(\cdot, \cdot)$ are subscripted by k since their hyperparameters are allowed to be different across the K experts. Any valid kernel function can be used. Let $\boldsymbol{\theta}_k$ be the vector with all the hyperparameters in the mean and kernel function of the GP prior.

The decision maker wants to compute the posterior distribution of the local ELPD $\eta_k(\tilde{\mathbf{z}}) = \mathbb{E}_{p_*}(\tilde{\ell}_k) = a_{ik} - b_k(1 + \lambda_k(\tilde{\mathbf{z}}))$ at a new point $\tilde{\mathbf{z}}$ in pooling space for each expert. This is achieved by sampling from the joint posterior

$$p(\lambda_k(\tilde{\mathbf{z}}), \boldsymbol{\lambda}_k, b_k, \boldsymbol{\theta}_k \mid \boldsymbol{\ell}'_k), \tag{9}$$

where $\boldsymbol{\ell}'_k = (\ell'_{1k}, \dots, \ell'_{nk})^\top$ and $\boldsymbol{\lambda}_k = (\lambda_k(\mathbf{z}_1), \dots, \lambda_k(\mathbf{z}_n))^\top$ is the vector of non-centrality parameters in the training data. We sample the potentially high-dimensional posterior in (9) using Hamiltonian Monte Carlo (HMC) in Stan (Stan Development Team, 2022; Gabry and Češnovar, 2020).

2.4. Cube root transformed Gaussian process regression

HMC sampling for the scaled non-central χ^2 Gaussian process regression is efficient, but necessarily slow in even moderately large datasets since $\boldsymbol{\lambda}_k$ is high-dimensional. This subsection presents a cube root transformation of the log scores which makes the log scores approximately normal with constant variance. This allows us to analytically integrate out the high-dimensional latent ELPD surfaces from the posterior, thereby substantially speeding up the computation of the ELPD posterior at a new point in the pooling space. We will refer to this model in tables and figures as $\text{GP}(1/3)$.

Starting from the linear transformation $\ell'_{ik} = -(\ell_{ik} - a_{ik})$, we further transform the log scores ℓ'_{ik} by taking the cube root, which is motivated by Abdel-Aty (1954) who shows

that a version of the Wilson-Hilferty transformation of the χ_k^2 distribution approximately holds for $X \sim \chi_k^2(\lambda)$ as well. That is

$$\left(\frac{X}{k + \lambda}\right)^{1/3} \dot{\sim} \mathcal{N}, \quad (10)$$

where the mean and variance of the normal distribution depends on the non-centrality parameter λ as well as the degrees of freedom. Since the non-centrality parameter λ is not known, we use a plain cube-root $X^{1/3}$ transformation when transforming the log scores. Figure 2 shows that this transformation makes the log scores approximately Gaussian; compare with Figure 1. As λ goes towards infinity the variance goes to zero, but Figure 3 shows that the variance is approximately constant in a range of reasonable λ values. We use the notation ℓ'' for these twice transformed log scores.

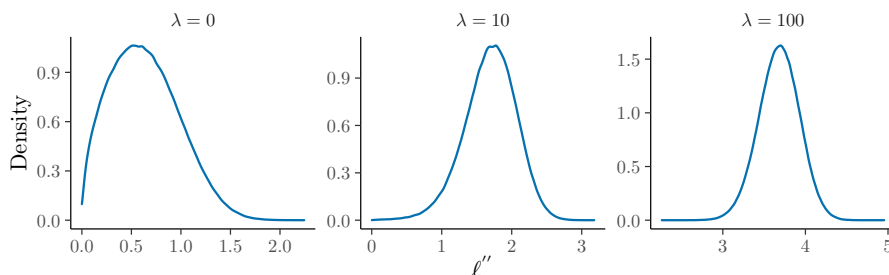


Figure 2: Approximate distribution of transformed log scores for a Gaussian expert and DGP with equal variance for three different $\lambda_k = (\mu_* - \mu_k)^2$.

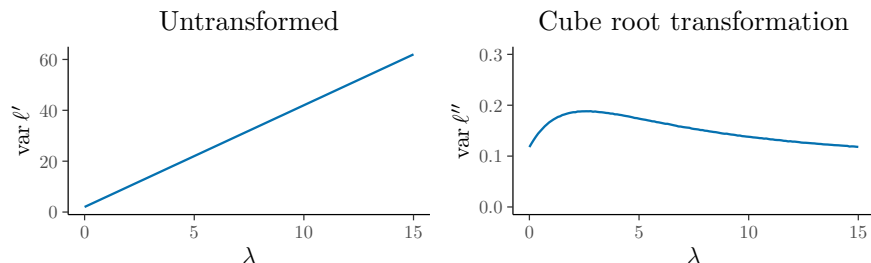


Figure 3: Variance of log scores as function of $\lambda = (\mu_* - \mu_k)^2$ for a Gaussian expert and DGP with equal variance.

Once our log scores have been transformed to approximate normality with constant variance, we can use a Gaussian process with homoscedastic Gaussian noise to model

the predictive ability of each expert:

$$\begin{aligned} \ell''_{ik} | f_k(\mathbf{z}_i), \sigma_k &\stackrel{\text{indep.}}{\sim} \mathcal{N}(f_k(\mathbf{z}_i), \sigma_k^2) \\ f_k(\mathbf{z}) &\sim \text{GP}(\mu_k(\mathbf{z}), g_k(\mathbf{z}, \mathbf{z}')) \\ \sigma_k^2 &\sim \mathcal{N}^+(0, \psi_\sigma^2). \end{aligned} \quad (11)$$

Again, let $\boldsymbol{\theta}_k$ denote the vector of hyperparameters in the mean and kernel functions of the GP for the k th expert.

Since $\ell_{ik} = a_{ik} - (\ell''_{ik})^3$, the ELPD at the test point $\tilde{\mathbf{z}}$ is $\eta_k(\tilde{\mathbf{z}}) = \tilde{a}_k - \mathbb{E}_{p_*} \left[\left(\tilde{\ell}''_k \right)^3 \right]$. For a general $X \sim \mathcal{N}(\mu, \sigma^2)$ we have

$$\mathbb{E}(X^3) = \mu^3 + 3\mu\sigma^2, \quad (12)$$

and hence

$$\begin{aligned} \mathbb{E}_{p_*} [(\tilde{\ell}''_k)^3] &= [\mathbb{E}_{p_*}(\tilde{\ell}''_k)]^3 + 3\mathbb{E}_{p_*}(\tilde{\ell}''_k) \cdot \text{var}_{p_*}(\tilde{\ell}''_k) \\ &= f_k^3(\tilde{\mathbf{z}}) + 3f_k(\tilde{\mathbf{z}})\sigma_k^2. \end{aligned} \quad (13)$$

We therefore have the following expression for the local ELPD at $\tilde{\mathbf{z}}$

$$\eta_k(\tilde{\mathbf{z}}) = \tilde{a}_k - f_k^3(\tilde{\mathbf{z}}) - 3f_k(\tilde{\mathbf{z}})\sigma_k^2 \quad (14)$$

To obtain the posterior for $\eta_k(\tilde{\mathbf{z}})$, we need the joint posterior $p(f_k(\tilde{\mathbf{z}}), \sigma_k, \boldsymbol{\theta}_k | \boldsymbol{\ell}''_k)$. Due to the approximate normality induced by the cube root transformation, we can analytically integrate out $\mathbf{f}_k = (f_k(\mathbf{z}_1), \dots, f_k(\mathbf{z}_n))^\top$ in the training data, and obtain the marginal posterior of σ_k and the kernel hyperparameters $\boldsymbol{\theta}_k$ in closed form (Rasmussen and Williams, 2006, Eq. 2.28)

$$p(\sigma_k, \boldsymbol{\theta}_k | \boldsymbol{\ell}''_k) = \int p(\mathbf{f}_k, \sigma_k, \boldsymbol{\theta}_k | \boldsymbol{\ell}''_k) d\mathbf{f}_k, \quad (15)$$

where $\boldsymbol{\ell}''_k$ is a vector with transformed log scores in the training data. This low-dimensional marginal posterior can be sampled with Hamiltonian Monte Carlo (HMC) using Stan (Stan Development Team, 2022; Gabry and Češnovar, 2020) in a fraction of the time that it takes to sample with full joint posterior for the $\text{GP}(\chi_1^2)$ model in (9).

For each HMC sampled $(\sigma_k, \boldsymbol{\theta}_k)$ we can now easily sample $f_k(\tilde{\mathbf{z}})$ from (Rasmussen and Williams, 2006)

$$f_k(\tilde{\mathbf{z}}) | \boldsymbol{\ell}''_k, \mathbf{Z}, \tilde{\mathbf{z}}, \sigma_k, \boldsymbol{\theta}_k \sim \mathcal{N}[\bar{f}(\tilde{\mathbf{z}}), \text{var}(f(\tilde{\mathbf{z}}))], \quad (16)$$

where \mathbf{Z} is the matrix with pooling variables in the training data, and

$$\begin{aligned} \bar{f}(\tilde{\mathbf{z}}) &= \mu_k(\tilde{\mathbf{z}}) + \mathbf{G}(\tilde{\mathbf{z}}, \mathbf{Z}) [\mathbf{G}(\mathbf{Z}, \mathbf{Z}) + \sigma_k^2 \mathbf{I}]^{-1} (\boldsymbol{\ell}''_k - \boldsymbol{\mu}_k), \\ \text{var}(f(\tilde{\mathbf{z}})) &= \mathbf{G}(\tilde{\mathbf{z}}, \tilde{\mathbf{z}}) - \mathbf{G}(\tilde{\mathbf{z}}, \mathbf{Z}) [\mathbf{G}(\mathbf{Z}, \mathbf{Z}) + \sigma_k^2 \mathbf{I}]^{-1} \mathbf{G}(\mathbf{Z}, \tilde{\mathbf{z}}), \end{aligned}$$

where, for example, $\mathbf{G}(\mathbf{Z}, \mathbf{Z})$ is the $n \times n$ matrix with covariances among the $f(\mathbf{z})$ in the training data given by the kernel function $g_k(\cdot, \cdot)$. The posterior draws of σ_k from (15) and $f_k(\tilde{\mathbf{z}})$ from (16) can finally be inserted into (14) to obtain draws from the posterior of the local ELPD $\eta_k(\tilde{\mathbf{z}})$. The procedure is summarized in Algorithm 1.

Algorithm 1: Sampling from the ELPD posterior in the GP (1/3) model

Input: Number of posterior draws M .

Generate M draws $\{\sigma_k^{(j)}, \boldsymbol{\theta}_k^{(j)}\}_{j=1}^M$ from $p(\sigma_k, \boldsymbol{\theta}_k | \ell_k'')$ in (15) using HMC.

for $j = 1, \dots, M$ **do**

 Sample from the posterior predictive $f_k^{(j)}(\tilde{\mathbf{z}}) | \ell_k'', \mathbf{Z}, \tilde{\mathbf{z}}, \sigma_k^{(j)}, \boldsymbol{\theta}_k^{(j)}$ in (16)

 Compute the ELPD draw: $\eta_k^{(j)}(\tilde{\mathbf{z}}) = a_{*k} - (f_k^{(j)}(\tilde{\mathbf{z}}))^3 - 3f_k^{(j)}(\tilde{\mathbf{z}})(\sigma_k^{(j)})^2$

end

Output: Sample from ELPD posterior: $\eta_k^{(1)}, \eta_k^{(2)}, \dots, \eta_k^{(M)}$.

2.5. General power-transformed Gaussian process regression

The cube root transformation is suitable when the log scores follow a scaled non-central χ_1^2 distribution, which is the correct model in the important case when both the DGP and the expert is Gaussian. Deviations from Gaussianity lead to new models that need to be derived on a case by case basis. The posterior distribution of the ELPD can be sampled with HMC as in the non-central χ_1^2 model described above. There may be new transformations that convert the log scores to something that can be modeled by a Gaussian process regression with Gaussian errors, but also this needs to be determined for each particular model.

Moderate departures from Gaussianity can however be handled with a more general power transformation than the cube root transformation. Let $\ell_{ik}^{(\alpha)} = (\ell_{ik}')^\alpha$ for $\alpha > 0$ be a general power transformation. The ELPD will then be $\eta_k(\tilde{\mathbf{z}}) = \tilde{a}_k - \mathbb{E}_{p_*} [(\tilde{\ell}_k^{(\alpha)})^{1/\alpha}]$. The fractional moments $\mathbb{E}_{p_*} [(\tilde{\ell}_k^{(\alpha)})^{1/\alpha}]$ can again be expressed in terms of $f_k(\tilde{\mathbf{z}})$ and σ_k^2 as in (14) using the formulas in Haldane (1942). The power parameter, α , can be sampled in the HMC step along with σ_k and the kernel hyperparameters in $\boldsymbol{\theta}_k$. The prior for α can be centered on $\alpha = 1/3$, i.e. the cube root transformation.

3. Simulation study

To explore the properties of our methods we implement them on simulated data. We are particularly interested in investigating how the computationally faster GP(1/3) model compares to the computationally costly GP(χ_1^2) model.

We generate data from the model

$$y_i = x_{1i} + x_{2i} + \epsilon_i, \quad \epsilon_i \stackrel{\text{iid}}{\sim} \mathcal{N}(0, 1), \quad (17)$$

where the covariates x_1 and x_2 are generated as i.i.d. standard normal variates. As our expert we use a Bayesian regression model that is misspecified in that one of the covariates is missing, i.e.

$$y_i = \alpha + \beta x_{1i} + \epsilon_i, \quad \text{where } \epsilon_i \stackrel{\text{iid}}{\sim} \mathcal{N}(0, \sigma_\epsilon). \quad (18)$$

To make the expert model as simple as possible for this illustration, we assume that it has been trained with so much data that the posterior of all coefficients will have variances close to zero and posterior means equal to 0 for α , 1 for β , and 2 for σ_i^2 (since ε_i absorbs both ϵ_i in the DGP and the variation from the missing x_{2i}).

We further assume that our decision maker believes that the predictive ability of the expert varies over the variable x_2 , but does not know the exact relationship between the ELDP η and x_2 . We will examine how well the decision maker will be able to estimate the true predictive ability, as summarized by the posterior distribution of η , using the two models described in Section 2.

The true distribution of the log scores in this setup is given by

$$\ell_i \stackrel{d}{=} -\frac{1}{2} \log 2\pi\sigma_i^2 - \frac{1}{2\sigma_i^2}(y_i - \mu_i)^2,$$

with each $y_i \mid x_{1i}, x_{2i} \stackrel{\text{indep.}}{\sim} \mathcal{N}(x_{1i} + x_{2i}, 1)$. For our expert $\mu_i = x_{1i}$ and $\sigma_i^2 = 2$, so this simplifies to

$$\ell_i \stackrel{d}{=} -\frac{1}{2} \log 4\pi - \frac{1}{4}(x_{2i} + \epsilon_i)^2.$$

As $x_{2i} + \epsilon \sim \mathcal{N}(x_{2i}, 1)$, it follows that $(x_{2i} + \epsilon)^2 \sim \chi_1^2(\lambda_i = x_{2i}^2)$, and the true ELPD over x_2 is given by

$$\eta(x_2) = \mathbb{E}(\ell \mid x_2) = -\frac{1}{2} \log 4\pi - \frac{1}{4}(1 + x_2^2).$$

Note that when $|x_2|$ is small, the distribution of ℓ is close to the central χ_1^2 distribution with a heavy tail to the right generating extreme values. As $|x_2|$ grows, the distribution approaches the normal distribution but the variance grows large. This shows that modeling log scores is a hard problem.

To compare the GP (χ_1^2) and GP (1/3) models we simulate 1000 data sets of 150 observations each from the DGP in Equation (17). For each simulation, we then generate draws from the posterior distribution of $\eta(x_2)$ over a grid of x_2 values between -3 and 3 , and compare with the true ELPD as a function of x_2 . Both GPs use a squared exponential kernel (Rasmussen and Williams, 2006). We use $l \sim \text{Inverse-Gamma}(5, 5)$ priors for the length scales, and a $\alpha \sim \mathcal{N}^+(0, 1)$ prior for the signal variances. The noise variance σ_n^2 of the GP(1/3) is given a $\mathcal{N}^+(0, 1)$ prior as well.

Figure 4 show the posterior mean of $\eta(x_2)$ together with a 95% credible interval for three different data sets. The data sets have been selected by ranking the mean integrated squared error (MISE) of the ELPD estimates of each run – the MSE integrated over the distribution of x_2 – and then selecting the 2.5:th, 50:th, and 97.5:th percentile. Both methods perform well for $x_2 \in (-2, 2)$, but poorly in the tails. This is to be expected, as two factors conspire to make estimation in the tails difficult: the DGP variance of the log scores increases with the square of x_2 , and since $x_2 \sim \mathcal{N}(0, 1)$ only roughly 5% of the observations are in the tails.

Figure 5 shows the difference in log MISE of the two models, and that the GP (1/3) model actually works marginally better in terms of squared error. However, the MISE

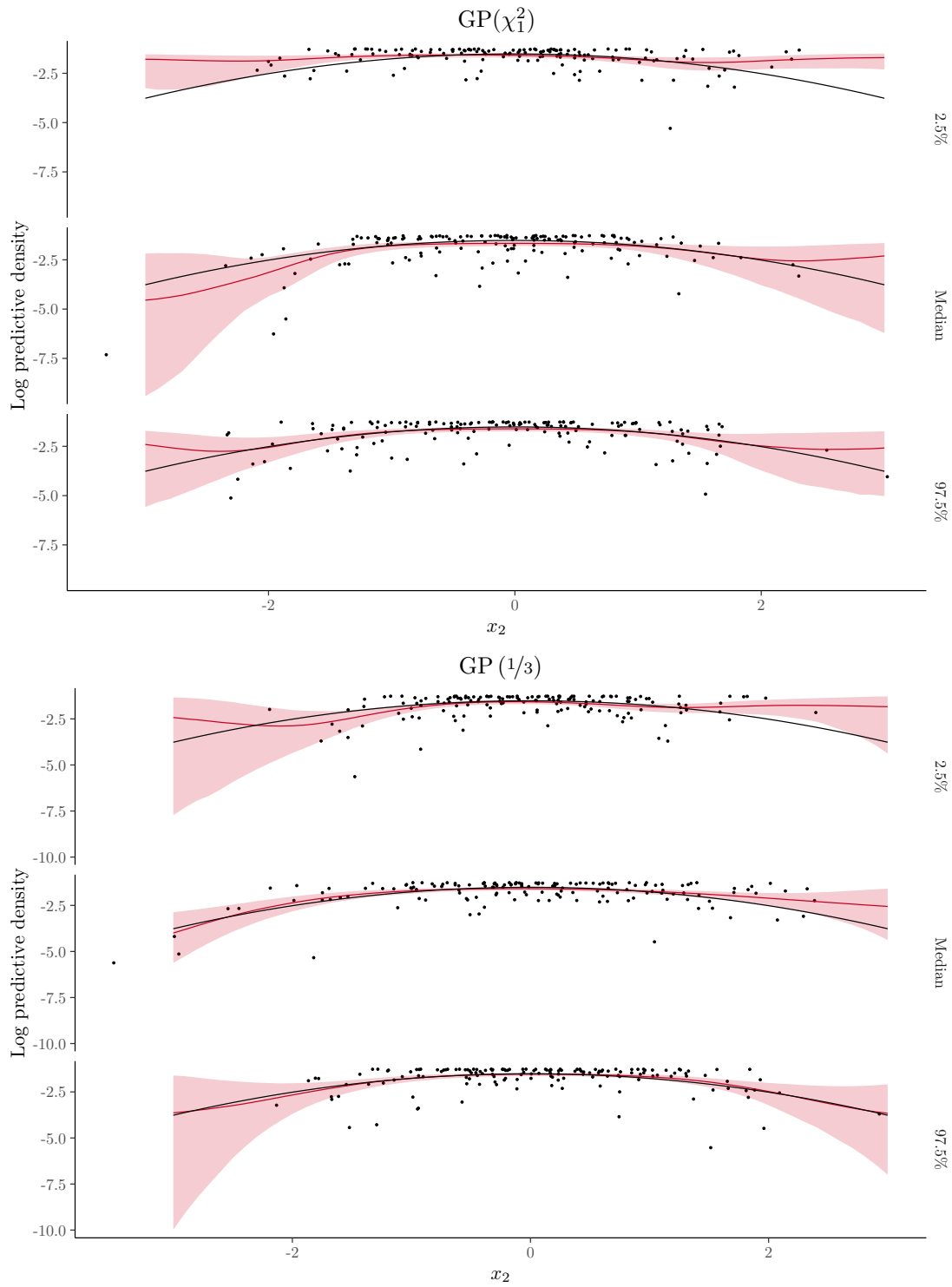


Figure 4: Posterior distribution of $\eta(x_2)$ over a grid of x_2 values for the $\text{GP}(\chi_1^2)$ (top) and $\text{GP}(1/3)$ (bottom) models. The black line is the true $\eta(x_2)$. The red line is the posterior median and the red ribbon is the 95% highest posterior density intervals. Median, 2.5%, and 97.5% indicates which sample, out of 1000, was used for each plot where the samples are ranked according to mean integrated squared error (MISE).

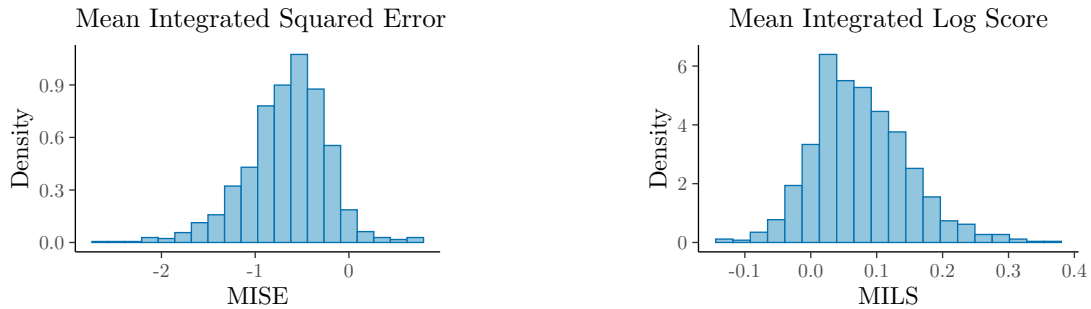


Figure 5: The left figure shows the difference in log mean integrated squared error (MISE) of the GP (1/3) and GP(χ_1^2) model, taken over the distribution of x_2 . The right figure shows the difference in mean integrated log score (MILS) of the GP(1/3) and GP(χ_1^2) model, taken over the distribution of x_2 .

metric only takes the posterior mean into account, so we also look at the mean integrated log score, which is calculated as the log predictive density of the true ELPD given the posterior distribution of $\eta(x_2)$, integrated over the distribution of x_2 . The GP (1/3) model works marginally better measured by this metric as well.

Note that the uncertainty around the estimate increases quickly for both models when there are no, or few, previous predictions nearby. This will lead to the positive behavior that when combining experts in regions where we have little to go on in terms of previous predictions, we will quickly tend towards an equal-weights solution; see Section 4.

The GP(χ_1^2) is prohibitively costly from a computational standpoint once the number of observations goes above a few hundred. The fact that the more scalable GP (1/3) model works so well compared to the GP(χ_1^2) model is therefore an important finding for practical applications. There is also a large collection of methods for reducing computational cost in GP regression with additive homoscedastic errors (Liu et al., 2020) that can be directly used to speed up inference in the GP (1/3) model.

4. Application to bike rental prediction

Rental services for bikes or similar vehicles is a large and growing business in many developed urban areas. An important task for such businesses is the prediction of vehicles usage, on a daily or more granular basis. This section applies the method described in Section 2 to estimate the local one-step-ahead predictive ability of three experts/models predicting bike rentals based on the data in Fanaee-T and Gama (2014). We then propose and implement a method for aggregating predictive distributions based on these estimates.

4.1. Inferring local predictive ability

The bike sharing dataset in Fanaee-T and Gama (2014) includes the daily number of rentals, our main variable of interest, from January 1, 2011 to December 31, 2012. To predict this variable, the experts use several covariates related to the weather, an indicator for season, and the number of bike rentals the previous day. They also use indicators for workday and holiday, the latter being based on a list of official US holidays.

We use the same setup as in Oelrich et al. (2021), with three experts: a Bayesian regression model (BREG), a Bayesian additive regression tree model (BART), and a Bayesian linear regression model with stochastic volatility (SVBVAR). For further discussion of the pooling variables and the data set, see Oelrich et al. (2021).

To estimate local predictive ability, we use the GP ($1/3$) method, as the number of data points makes the GP (χ_1^2) method inconveniently slow. More specifically, we use a GP with a squared exponential kernel with automatic relevance determination (ARD) so that each pooling variable is associated with its own length scale hyperparameter (Rasmussen and Williams, 2006). Following the Gaussian process regression example in the Stan User’s Guide, we give the length scales independent Inverse-Gamma(5, 5) priors, and the noise and signal variance are given $\mathcal{N}^+(0, 1)$ priors (Stan Development Team, 2022). Figure 6 shows the prior and posterior distribution of the length scales for all three experts at the final time point. The length scale tells us how quickly the correlation between two points decreases, so smaller length scales are indicative of greater locality, in the sense of local predictive ability varying more rapidly over the pooling space. *Temperature* and in particular *Family Day* show the strongest evidence of locality with a posterior that is heavily concentrated on smaller length scales. There is also some variation between the experts, with the Bayesian regression model showing more evidence of local behavior.

To illustrate how local predictive ability changes over the pooling space, Figure 8 shows the actual posterior of local predictive ability for Christmas Day 2012 together with what the posterior would have looked like if we keep all pooling variables constant except the value of *family day*. The BART model would, if this had not been a family day, be expected to perform roughly as well as the Bayesian regression model, with the stochastic volatility expected to have the poorest performance. However, for *family day* = 1, which is what was observed, the model expects the stochastic volatility model to perform well and the BART to have the worst local predictive ability by a wide margin.

Figure 7 shows a 95% highest posterior density (HPD) interval for the predictive distribution of a subset of the log scores; see Appendix A for results for the full dataset. For all experts, the majority of observed log scores land within the HPD. However, around twice as many as would be expected fall outside, with BART doing the worst and SVBVAR the best. This may indicate that the decision maker could be missing an important pooling variable.

Table 1 evaluates the quality of the one-step-ahead predictions of local predictive

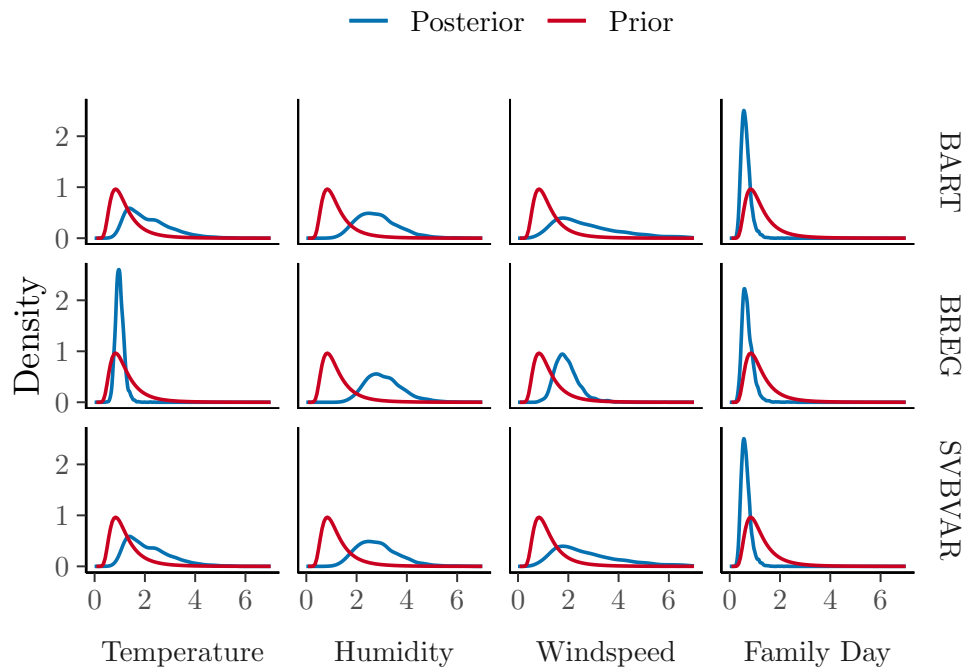


Figure 6: Marginal posterior and prior distributions of the length scales for all three experts at the final time point.

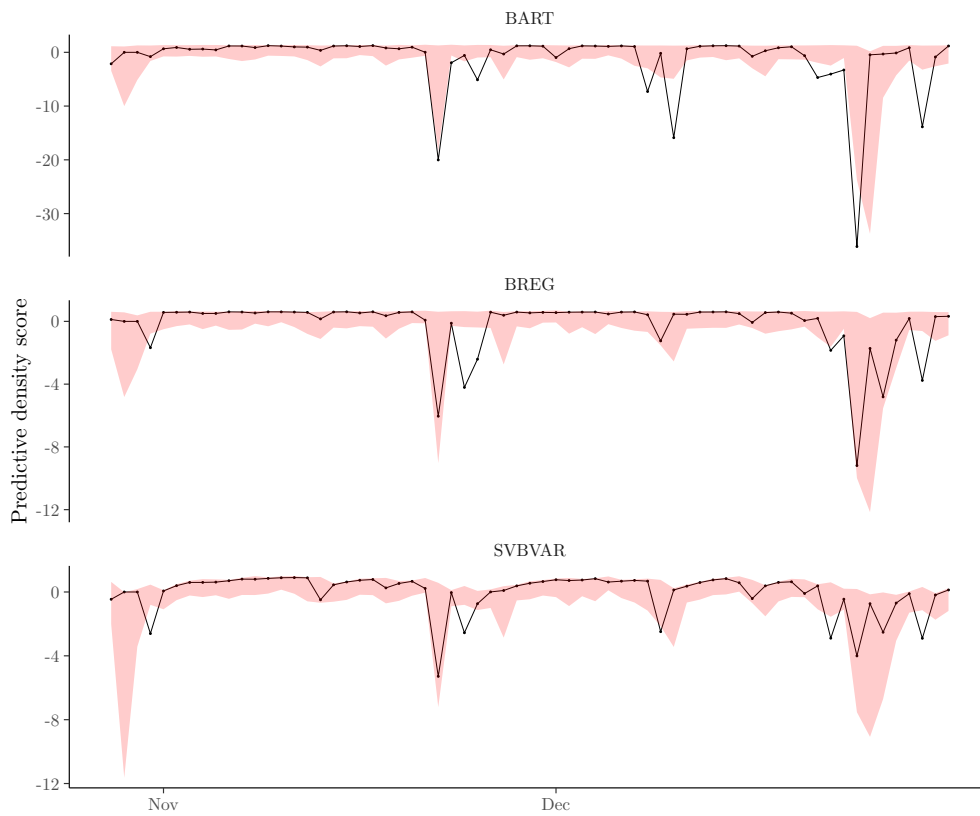


Figure 7: Estimates of local predictive ability for a subset of the bike sharing data. The black line shows the observed log scores and the red ribbon shows a 95% HPD interval for the posterior predictive distribution of log scores. See Appendix A for plots of the full data set.

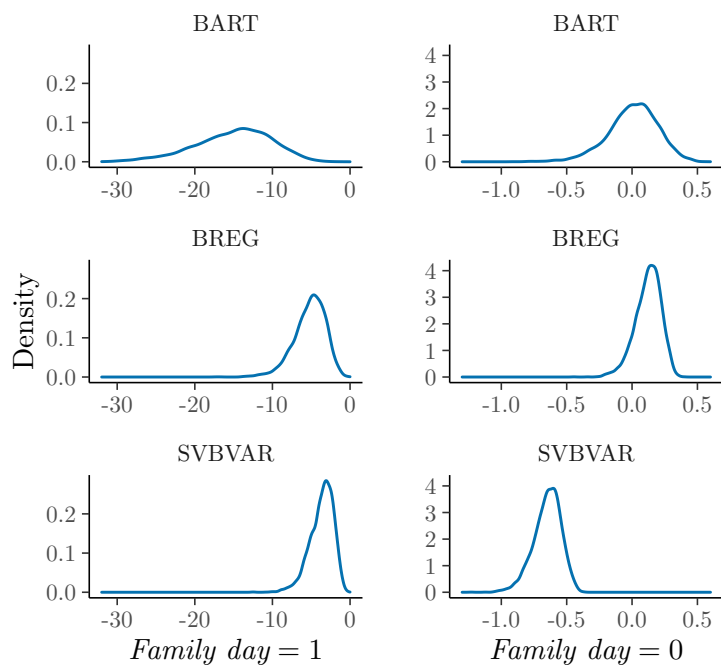


Figure 8: The left side shows the posterior distribution of local predictive ability for Christmas Day 2012. The right side shows the same distribution but with *family day* set to 0.

Expert	Method	Median	Mean
BART	ℓ' random walk	-1.80	-3.14
	ℓ' cumulative mean	-1.83	-2.62
	ℓ'' random walk	-0.20	-0.58
	ℓ'' cumulative mean	-0.07	-0.42
	GP(1/3)	0.02	-2.10
BREG	ℓ' random walk	-1.08	-1.80
	ℓ' cumulative mean	-1.11	-1.54
	ℓ'' random walk	0.23	-0.03
	ℓ'' cumulative mean	0.44	0.13
	GP(1/3)	0.58	-3.67
SVBVAR	ℓ' random walk	-1.38	-1.81
	ℓ' cumulative mean	-1.40	-1.61
	ℓ'' random walk	0.19	-0.14
	ℓ'' cumulative mean	0.58	0.20
	GP(1/3)	0.68	-2.27

Table 1: Mean and median log predictive score of one-step-ahead predictions of log scores. See (19) for a description of the models.

ability from the GP(1/3) model and compares it with four benchmark models:

$$\begin{aligned}
\ell' \text{ random walk} : \quad & \ell'_{ik} \mid \ell'_{i-1,k} \sim \mathcal{N}(\ell'_{i-1,k}, \sigma^2) \\
\ell' \text{ global mean} : \quad & \ell'_{ik} \sim \mathcal{N}(\mu, \sigma^2) \\
\ell'' \text{ random walk} : \quad & \ell''_{ik} \mid \ell''_{i-1,k} \sim \mathcal{N}(\ell''_{i-1,k}, \sigma^2) \\
\ell'' \text{ global mean} : \quad & \ell''_{ik} \sim \mathcal{N}(\mu, \sigma^2), \tag{19}
\end{aligned}$$

where all models are finally transformed to predict the original log scores ℓ_{ik} . Table 1 shows that the two reference methods based on the linearly transformed log scores ℓ' perform badly across the board, giving additional support to the cube root transformation. The global model based on power-transformed log scores is the best performer in terms of the mean, but GP(1/3) outperforms it when it comes to the median. This discrepancy between mean and median is due to a few extreme outliers, the worst being a log score of roughly -700 .

Figure 9 shows how well the power-transformed benchmark models and the GP(1/3) model predicts the observed log scores for each expert. The figure shows (kernel density estimates of) the log density of all observed log scores, $\log p(\ell_{i+1} \mid \ell_{1:i})$, in the test data, with respect to each local ELPD model. The median of each distribution is marked out with a red vertical line. We see that the GP(1/3) model performs better on a majority of the observations, but has a longer left tail caused by a very low predictive density for some observed log scores.

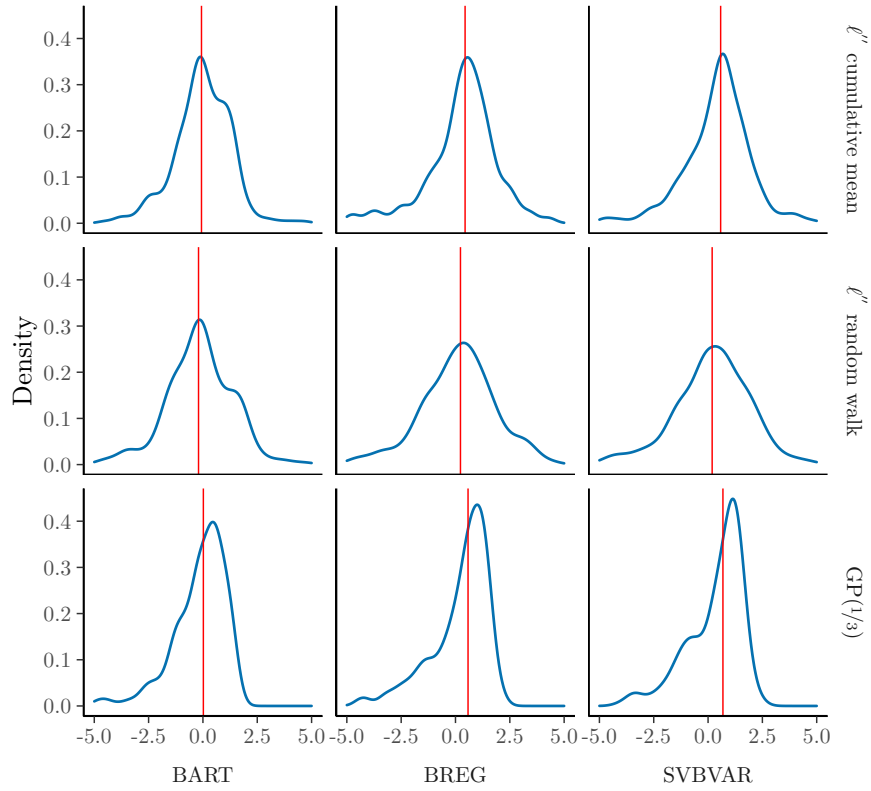


Figure 9: Kernel density estimates of one-step-ahead log density evaluations of the predicted log scores, $\log p(\ell_{i+1} \mid \ell_{1:i})$, in the test data for the bike rental data. The rows in the figure corresponds to predictions from the GP(1/3) model and two global reference methods, respectively. The median of each distribution is marked out with a red vertical line.

4.2. Using local predictive ability for forecast combination

Inferred local predictive ability has a natural use when combining expert forecasts. A natural approach is to weigh each expert directly by the posterior probability that the predictive ability of that expert is greater than all other experts, $p(\eta_k(\tilde{\mathbf{z}}) > \eta_{j \neq k}(\tilde{\mathbf{z}}))$. In practice however, when the amount of data is small these weights will tend to not discriminate strongly enough between experts and be outperformed by more aggressive weighing schemes, which leads us to consider other methods. As a flexible aggregation weights based on local predictive ability we propose feeding $p(\eta_k(\tilde{\mathbf{z}}) > \eta_{j \neq k}(\tilde{\mathbf{z}}))$ through a softmax transformation

$$w_k(\tilde{\mathbf{z}}) = \frac{\exp\left(c \times p(\eta_k(\tilde{\mathbf{z}}) > \eta_{j \neq k}(\tilde{\mathbf{z}}))\right)}{\sum_{k=1}^K \exp\left(c \times p(\eta_k(\tilde{\mathbf{z}}) > \eta_{j \neq k}(\tilde{\mathbf{z}}))\right)}. \quad (20)$$

The constant c , which we will refer to as the discrimination factor, allows the decision maker to tune how aggressively to discriminate between the experts. Setting $c = 0$ will result in equal weights, and setting $c = \infty$ will assign weight one to the expert with the highest probability of having greater predictive ability than all other experts. Typically a value of c between these extremes will yield the best results.

When the decision maker has no strong prior opinion of c , it can be dynamically selected at each time point by selecting the value that optimizes the historical predictive ability of the pool. We refer to this method as GP(1/3) *dynamic* in tables and figures.

Two alternatives to this method that we will use as benchmarks is to simply weigh by the posterior probability $p(\eta_k(\tilde{\mathbf{z}}) > \eta_{j \neq k}(\tilde{\mathbf{z}}))$, or to assign weight one to the model with the highest posterior expectation of $\eta(\tilde{\mathbf{z}})$. We will refer to these two variants in tables and figures as GP(1/3) *natural* and GP(1/3) *model selection*, respectively.

Figure 10 shows how the optimal discrimination changes over time for the bike share data. At each time point, the historical performance of the pool for $0 \leq c \leq 20$ is evaluated, and the next prediction is made with the value of c corresponding to the historically most accurate pool. The optimal discrimination c is volatile when little historical data is available, but then settles down around $c = 5$ as a compromise between the extremes of equal weights and assigning all weight to the expert with highest probability of having the best predictive ability at $\tilde{\mathbf{z}}$.

Figure 11 shows the cumulative log predictive density for the three methods. The dynamic method perform best, closely followed by the selection method.

Figure 12 compares the best performing of the GP(1/3) methods with a selection of reference methods: the caliper method used in Oelrich et al. (2021), which is a non-parametric method that averages log scores of nearby observations in \mathbf{z} -space; the global optimal pool of Geweke and Amisano (2011) which selects aggregation weights that optimize the historical performance of the pool in terms of log scores; the local optimal pool in Oelrich et al. (2021), which is an extension of the optimal pool of Geweke and Amisano (2011) where the optimal weights are determined on a subset of the data in the pooling space closest to the current point. For more detail about these reference methods, see Oelrich et al. (2021). Figure 12 shows that the GP(1/3) initially struggles

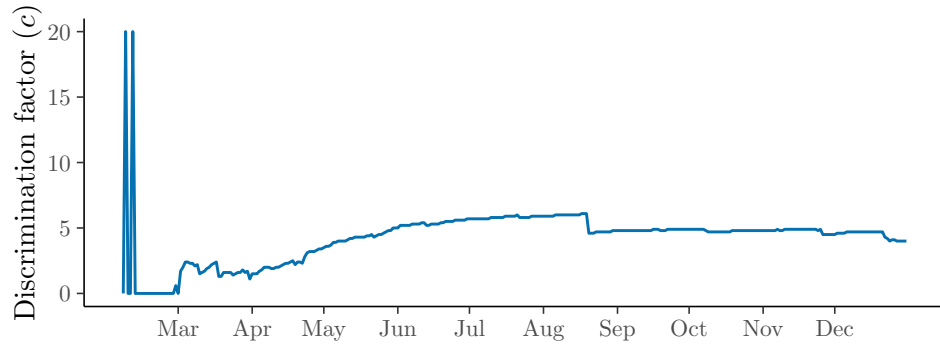


Figure 10: Optimal value of the discrimination factor c in (20) over time in the bike rental data.

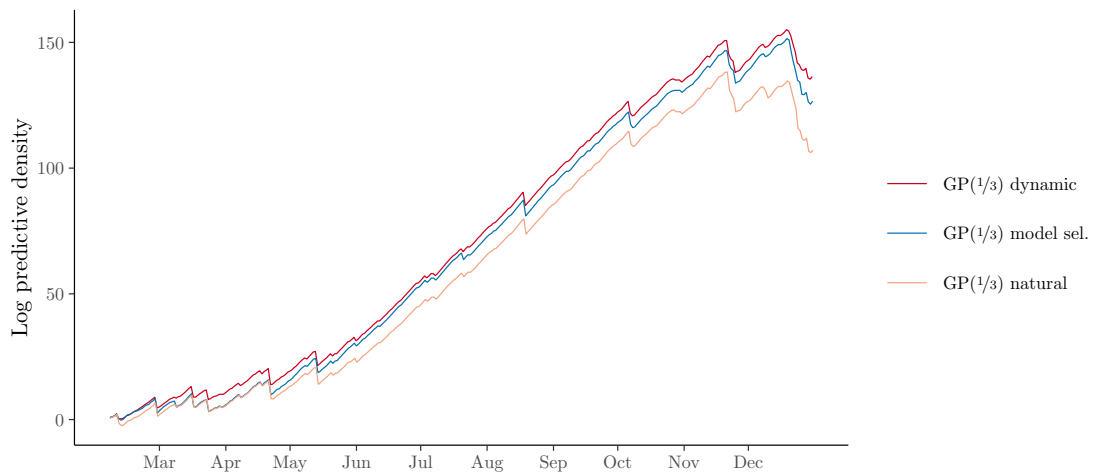


Figure 11: Cumulative log predictive density for three methods based on local predictive ability. The legend is sorted in descending order of total log predictive score.

when there is little training data, but then quickly improves over time and at the end of the sample it only beaten by the local optimal pool. The total sums for all methods, together with the performance of the individual experts, are shown in Table 2.

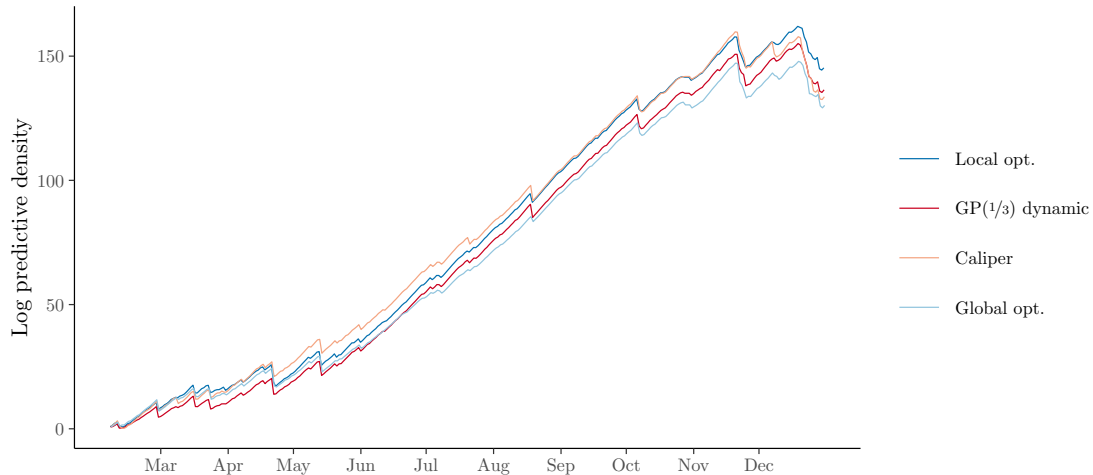


Figure 12: Cumulative log predictive density for the four best methods. The legend is sorted in descending order of total log predictive score.

5. Conclusions and further research

We have introduced a method for estimating the predictive ability $\eta(\mathbf{z})$ of a model or expert, in terms of ELPD, as it varies over a space of pooling variables \mathbf{z} . We call this conditional predictive ability *local predictive ability*, and propose using a Gaussian process to model it.

Gaussian processes have the drawback of being computationally heavy, and so we suggest the use of a power transformation of log scores which allows us to use a much faster marginalized GP to generate draws from the posterior of $\eta(\mathbf{z})$. Our proposed method is shown to work well for predicting bike share data (Fanaee-T and Gama, 2014), where it outperforms all compared methods except the local version of the linear prediction pool of Geweke and Amisano (2011) in Oelrich et al. (2021).

Our method models the marginal distribution of the predictive ability $\eta_k(\mathbf{z})$ for each expert. Extending the method to model the predictive ability of the experts jointly,

Method	Sum of log scores
SVBVAR	45.06
BREG	28.76
BART	43.64
Equal weights	98.65
Caliper	133.66
Global opt.	130.15
Local opt.	145.27
GP(1/3) natural	107.12
GP(1/3) model sel.	126.62
GP(1/3) dynamic	136.44

Table 2: Sum of log predictive density scores over the whole test period.

for example using a multi-output GP, is a natural extension, and is likely to have an impact on the pooling of experts (Winkler, 1981). Further work should also explore the properties of the general power transformed Gaussian process model proposed here, as well as deriving the distribution of log scores under different assumptions of expert distribution and data generating processes.

Our paper focuses on the effect of pooling variables and therefore deliberately ignores any persistence of local predictive ability over time. Allowing for time-varying weights is shown in Del Negro et al. (2014); Billio et al. (2013); McAlinn et al. (2020) to be beneficial in macroeconomic forecasting. While it is straightforward to include some function of time in the vector of pooling variables in our framework, some care should be taken to define an appropriate kernel function with respect to time.

Appendices

A. Estimates of local predictive ability

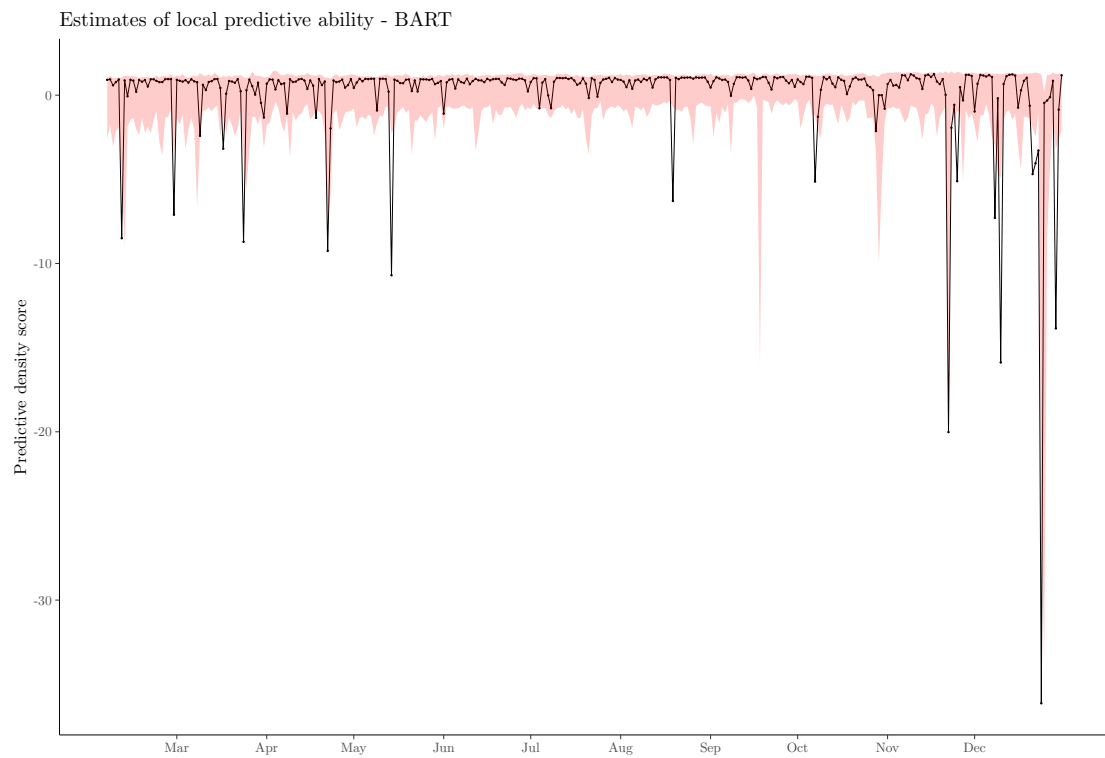


Figure 13: Estimates of local predictive ability for the BART model. The black line shows the observed log scores and the red ribbon shows a 95% HPD interval for the posterior predictive distribution of log scores.

References

- Abdel-Aty, S. H. (1954). Approximate Formulae for the Percentage Points and the Probability Integral of the Non-Central chi² Distribution. *Biometrika*, 41(3/4):538.
- AMS Council (2008). Enhancing weather information with probability forecasts. *Bull. Amer. Meteor. Soc.*, 89:1049–1053.

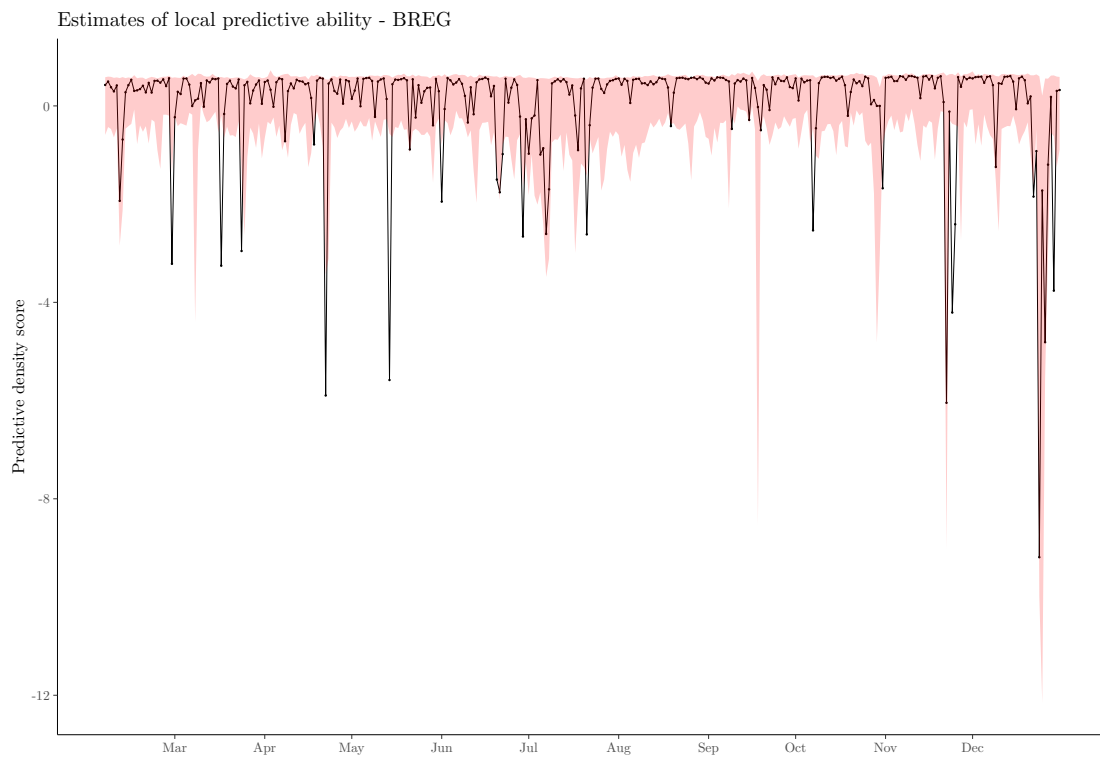


Figure 14: Estimates of local predictive ability for the BREG model. The black line shows the observed log scores and the red ribbon shows a 95% HPD interval for the posterior predictive distribution of log scores.

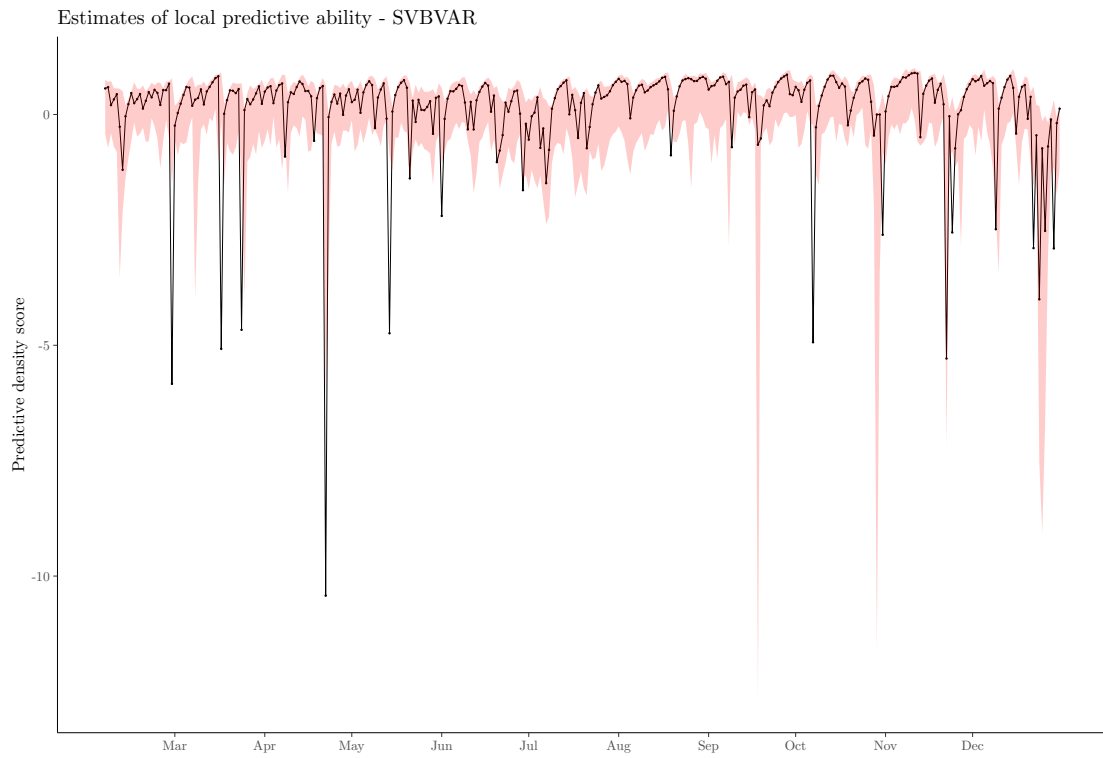


Figure 15: Estimates of local predictive ability for the SVBVAR model. The black line shows the observed log scores and the red ribbon shows a 95% HPD interval for the posterior predictive distribution of log scores.

- Bates, J. M. and Granger, C. W. J. (1969). The Combination of Forecasts. *Journal of the Operations Research Society*, 20(4):451–468.
- Billio, M., Casarin, R., Ravazzolo, F., and van Dijk, H. K. (2013). Time-varying combinations of predictive densities using nonlinear filtering. *Journal of Econometrics*, 177(2):213–232.
- Croushore, D., Stark, T., et al. (2019). Fifty years of the survey of professional forecasters. *Economic Insights*, 4(4):1–11.
- de Vincent-Humphreys, R., Dimitrova, I., Falck, E., Henkel, L., Meyler, A., et al. (2019). Twenty years of the ecb survey of professional forecasters. *Economic Bulletin Articles*, 1.
- Del Negro, M., Hasegawa, R., and Schorfheide, F. (2014). Dynamic Prediction Pools: An Investigation of Financial Frictions and Forecasting Performance. *Journal of Econometrics*, 192(2):391–405.
- Fanaee-T, H. and Gama, J. (2014). Event labeling combining ensemble detectors and background knowledge. *Progress in Artificial Intelligence*, 2(2-3):113–127.
- Gabry, J. and Češnovar, R. (2020). CmdStanR: R interface to 'cmdstan'. See mc-stan.org/cmdstanr/reference/cmdstanr-package.
- Gelman, A., Hwang, J., and Vehtari, A. (2014). Understanding predictive information criteria for Bayesian models. *Statistics and Computing*, 24(6):997–1016.
- Geweke, J. and Amisano, G. (2011). Optimal prediction pools. *Journal of Econometrics*, 164(1):130–141.
- Gneiting, T. and Raftery, A. E. (2007). Strictly Proper Scoring Rules, Prediction, and Estimation. *Journal of the American Statistical Association*, 102(477):359–378.
- Haldane, J. B. S. (1942). Moments of the Distributions of Powers and Products of Normal Variates. *Biometrika*, 32(3/4):226.
- Hall, S. and Mitchell, J. (2007). Combining density forecasts. *International Journal of Forecasting*, 23(1):1–13.
- Li, L., Kang, Y., and Li, F. (2021). Feature-based Bayesian forecasting model averaging. Preprint. arXiv: 2108.02082.
- Lindley, D. V., Tversky, A., and Brown, R. V. (1979). On the Reconciliation of Probability Assessments. *Journal of the Royal Statistical Society: Series A (General)*, 142(2):146–180.
- Liu, H., Ong, Y.-S., Shen, X., and Cai, J. (2020). When gaussian process meets big data: A review of scalable gps. *IEEE transactions on neural networks and learning systems*, 31(11):4405–4423.

- McAlinn, K., Aastveit, K. A., Nakajima, J., and West, M. (2020). Multivariate Bayesian Predictive Synthesis in Macroeconomic Forecasting. *Journal of the American Statistical Association*, 115(531):1092–1110.
- Neal, R. M. (1996). *Bayesian learning for neural networks*. Number 118 in Lecture notes in statistics. Springer, New York.
- Oelrich, O., Villani, M., and Ankargren, S. (2021). Local Prediction Pools. arXiv:2112.09073 [math, stat].
- Rasmussen, C. E. and Williams, C. K. I. (2006). *Gaussian processes for machine learning*. MIT Press, Cambridge, Mass.
- Sivula, T., Magnusson, M., Matamoros, A. A., and Vehtari, A. (2022a). Uncertainty in Bayesian Leave-One-Out Cross-Validation Based Model Comparison. arXiv:2008.10296 [stat].
- Sivula, T., Magnusson, M., and Vehtari, A. (2022b). Unbiased estimator for the variance of the leave-one-out cross-validation estimator for a Bayesian normal model with fixed variance. arXiv:2008.10859 [stat].
- Stan Development Team (2022). Stan Modeling Language Users Guide and Reference Manual, version 2.30.
- Winkler, R. L. (1981). Combining Probability Distributions from Dependent Information Sources. *Management Science*, 27(4):479–488.
- Yao, Y., Pirš, G., Vehtari, A., and Gelman, A. (2021). Bayesian Hierarchical Stacking: Some Models Are (Somewhere) Useful. *Bayesian Analysis*. Advance online publication. doi:10.1214/21-BA1287.
- Yao, Y., Vehtari, A., Simpson, D., and Gelman, A. (2018). Using Stacking to Average Bayesian Predictive Distributions (with Discussion). *Bayesian Analysis*, 13(3):917–1007.